Glycan-foraging systems reveal the adaptation of Capnocytophaga canimorsus to the dog mouth

Renzi, Francesco; Manfredi, Pablo; Dol, Mélanie; Fu, Jian; Vincent, Stéphane; Cornelis, Guy Richard

Published in:
mBio

DOI:
10.1128/mBio.02507-14

Publication date:
2015

Document Version
Publisher's PDF, also known as Version of record

RESEARCH ARTICLE

Glycan-Foraging Systems Reveal the Adaptation of *Capnocytophaga canimorsus* to the Dog Mouth

Francesco Renzi,[a] Pablo Manfredi,[b] Mélanie Dol,[a] Jian Fu,[c] Stéphane Vincent,[c] Guy Richard Cornelis[a]

Département de Biologie, Université de Namur, Namur, Belgium[a]; Biozentrum der Universität Basel, Basel, Switzerland[b]; Département de Chimie, Université de Namur, Namur, Belgium[c]

ABSTRACT ***Capnocytophaga canimorsus* is known to form two kinds of cells on blood agar plates (coccoid and bacillary), evoking phase variation. When grown in coculture with animal cells these bacteria appeared only as bacilli, but in the presence of vancomycin they were round, indicating that coccoid shapes likely result from weakening of the peptidoglycan layer. Polysaccharide utilization locus 5 (*PUL5*) and sialidase mutant bacteria, unable to retrieve glycans from glycoproteins, grew less than wild-type bacteria and also appeared polymorphic unless GlcNAc was added, suggesting that *C. canimorsus* is unable to synthesize GlcNAc, an essential component of peptidoglycan. Accordingly, a genome analysis was conducted and revealed that *C. canimorsus* strain 5 lacks the GlmM and GlmU enzymes, which convert glucosamine into GlcNAc. Expression of the *Escherichia coli* GlmM together with the acetyltransferase domain of GlmU allowed *PUL5* mutant bacteria to grow normally, indicating that *C. canimorsus* is a natural auxotroph that relies on GlcNAc harvested from the host N-glycoproteins for peptidoglycan synthesis. Mucin, a heavily O-glycosylated protein abundant in saliva, also rescued growth and the shape of *PUL5* mutant bacteria. Utilization of mucin was found to depend on Muc, a Sus-like system encoded by *PUL9*. Contrary to all known *PUL*-encoded systems, Muc cleaves peptide bonds of mucin rather than glycosidic linkages. Thus, *C. canimorsus* has adapted to build its peptidoglycan from the glycan-rich dog's mouth glycoproteins.**

IMPORTANCE ***Capnocytophaga canimorsus* is a bacterium that lives as a commensal in the dog mouth and causes severe infections in humans. *In vitro*, it forms two kinds of cells (coccoid and bacillary), evoking phase variation. Here, we show that cell rounding likely results from weakening of the peptidoglycan layer due to a shortage of *N*-acetylglucosamine (GlcNAc). *C. canimorsus* cannot synthesize GlcNAc because of the lack of key enzymes. In its niche, the dog mouth, *C. canimorsus* retrieves GlcNAc by foraging glycans from salivary mucin and N-linked glycoproteins through two different apparatuses, Muc and Gpd, both of which are related to the *Bacteroides* starch utilization system. The Muc system is peculiar in the sense that the enzyme of the complex is a protease and not a glycosylhydrolase, as it cleaves peptide bonds in order to capture glycan chains. This study provides a molecular genetic demonstration for the complex adaptation of *C. canimorsus* to its ecological niche, the oral cavity of dogs.**

Received 17 January 2015 **Accepted** 23 January 2015 **Published** 3 March 2015

Citation Renzi F, Manfredi P, Dol M, Fu J, Vincent S, Cornelis GR. 2015. Glycan-foraging systems reveal the adaptation of *Capnocytophaga canimorsus* to the dog mouth. mBio 6(2):e02507-14. doi:10.1128/mBio.02507-14.

Editor R. John Collier, Harvard Medical School

Address correspondence to Guy Richard Cornelis, guy.cornelis@unamur.be.

This article is a direct contribution from a Fellow of the American Academy of Microbiology.

Capnocytophaga canimorsus is a capnophylic gliding Gram-negative bacterium from the *Bacteroidetes* phylum that is part of the normal flora of the dog mouth (1–5). Although it has not been reported to cause infections in dogs, it causes rare but severe infections in humans who are in contact with dogs (6, 7). The usual syndrome is septicemia, with mortality in the range of 50%. Patients are generally older than 40 years old, and roughly half of them have had a splenectomy or abused alcohol. However, the other half have had no medical history (for review, see references 8 to 10). *C. canimorsus* 5, a strain isolated from a patient with septic shock (11), has a lipopolysaccharide that triggers little inflammation (2, 11–13) and confers significant resistance to phagocytosis (2), antimicrobial peptides (12), and complement killing (2). Its genome, which consists of a single 2.5-Mb replicon (14), contains 13 so-called polysaccharide utilization loci (PUL) (15), a hallmark of *Bacteroidetes* bacteria (16). PUL typically encode polysaccharide-harvesting complexes made of several lipoproteins anchored in the outer membrane and that face the outside of the cell, as well as a TonB-dependent transporter. Some lipoproteins are devoted to glycan binding, while others are specific hydrolases. The archetype of such complexes is the *Bacteroides thetaiotaomicron* starch utilization system (Sus), initially described by Salyers and colleagues (17–20). *C. canimorsus* grows readily on blood agar plates and in coculture with animal cells but, surprisingly, it does not grow as well in the absence of animal cells or when it is separated from animal cells by a membrane, indicating that it relies on cells for nutrition (21). Unexpectedly, *C. canimorsus* does not damage the cells but instead deglycosylates the cellular

surface-exposed N-glycoproteins via its Gpd complex, encoded by *PUL5* (15, 21, 22). The Gpd complex consists of a SusC-like porin (GpdC), a SusD-like binding protein (GpdD), two ancillary lipoproteins (GpdEF), and an endo-β-*N*-acetylglucosaminidase (GpdG) which cleaves the N-linked oligosaccharide after the first *N*-acetylglucosamine (GlcNAc) residue (22). The Gpd complex deglycosylates not only surface glycoproteins but also soluble glycoproteins, like human IgG (22) and transferrin (23). Deglycosylation is required for growth in coculture with animal cells but also for survival in the mouse (15, 21). In the initial description of the species, Brenner et al. (1) reported that *C. canimorsus* cultivated on blood agar plates appeared as bacilli but also in different forms, including longer rods, filaments that are often curved, spindle shaped, and coccoid (1), which suggests that *C. canimorsus* undergoes some form of phase variation.

In the present manuscript, we show that *C. canimorsus* 5 is a natural auxotroph for GlcNAc that is missing the *glmM* and *glmU* genes, which enable bacteria to convert glucosamine into GlcNAc. The lack of GlcNAc leads to impaired peptidoglycan (PG) assembly and bacterial death, explaining the polymorphism seen on blood agar plates in the original description of the species (1). *C. canimorsus* harvests GlcNAc not only from host N-linked glycoproteins through the *PUL5*-encoded Gpd complex but also from mucin through the *PUL9*-encoded Muc complex. We propose that the GlcNAc auxotrophy, which contributes to virulence (21), results from the adaptation of *C. canimorsus* as a commensal of the glycan-rich dog mouth.

RESULTS

***C. canimorsus* polymorphism is due to *N*-acetylglucosamine starvation.** As reported early on (1), wild-type (wt) *C. canimorsus* 5 bacteria grown for 2 days on blood agar plates have different morphologies, ranging from filaments to coccoid forms (Fig. 1A). The coccoid forms strongly resemble the cells formed by *Escherichia coli* mutant strains that are unable to synthesize aminosugars (24). When glucosamine or GlcNAc is not provided in the medium, these mutants cannot synthesize glucosamine-6-P, and they form spheroplasts due to a reduction in PG synthesis (24). We thus speculated that the polymorphism observed with *C. canimorsus* 5 could be due to a similar reason. In order to see whether this alteration of cell morphology was due to aminosugar starvation and not some kind of phase variation, we supplemented the blood agar plates with 0.005% GlcNAc. As shown in Fig. 1A, the addition of GlcNAc significantly reduced the formation of abnormal forms, indicating that aminosugar starvation, rather than phase variation, could be responsible for the observed polymorphism of wt *C. canimorsus* bacteria grown on blood agar plates.

***PUL5* mutants grown on HEK293 cells are polymorphic due to a defect in peptidoglycan synthesis.** In coculture with HEK293 cells, *C. canimorsus* 5 bacteria deprived of the *PUL5*-encoded Gpd complex reach a biomass that is 10-fold lower than that of wt *C. canimorsus* 5 bacteria (15, 22) (Fig. 1B). Since this growth defect can be rescued by supplementation of the medium with GlcNAc (15) (Fig. 1B), we hypothesized it could mimic the growth defect of wt bacteria on blood agar plates, and we examined the morphology of wt and *PUL5* mutant bacteria after 24 h of coculture with HEK293 cells. Interestingly, while wt bacteria showed a bacillary form, *PUL5* mutants appeared elongated, enlarged, or completely round (Fig. 1C). As shown in Fig. S1A and B in the supplemental material, *PUL5* mutants progressively changed their morphology while they stopped dividing, suggesting that growth arrest and aberrant morphology are two linked phenomena. In contrast, in the presence of GlcNAc, *PUL5* mutant bacteria had the same morphology as wt bacteria (Fig. 1C), suggesting that GlcNAc starvation affects PG biosynthesis. In order to see whether a defect in PG biosynthesis determines the same growth arrest and cell rounding, we added vancomycin (25) in the coculture of HEK293 cells and wt *C. canimorsus* 5. As shown in Fig. 1D (see also Movie S1 in the supplemental material), the addition of vancomycin transformed wt *C. canimorsus* 5 bacteria into round cells, similar to those observed with *PUL5* mutant bacteria (see Movie S2 in the supplemental material). These results suggest that *PUL5* mutant bacteria, which cannot harvest host N-linked glycans, stop growing and change their cell shape because starvation of aminosugars leads to defects in peptidoglycan synthesis.

Sialidase mutants also have a peptidoglycan synthesis defect. The *PUL5*-encoded Gpd complex works in concert with a periplasmic sialidase (SiaC) whose activity is crucial for the subsequent processing of the cleaved glycan chains (22). Since a *siaC* deletion mutant also shows reduced growth on HEK293 cells which can be rescued by addition of aminosugars (21), we asked whether the bacterial cell shape of a *siaC* mutant would also be affected. Indeed, a *siaC* mutant cocultivated with HEK293 cells for 24 h also showed aberrant morphologies: elongated, enlarged, and completely round (Fig. 1E). Addition of GlcNAc restored the normal cell shape (Fig. 1E). We concluded from this result that the inability to metabolize host N-linked glycans, due to either blockade of glycan chain cleavage and import (*PUL5* deletion) or blockade of the first step of glycan processing in the periplasm (*siaC* deletion), results in aminosugar starvation. This starvation is likely to affect PG synthesis, leading to the appearance of aberrant cell shapes and growth arrest.

***C. canimorsus* 5 is missing the genes *glmM* and *glmU*.** Since *C. canimorsus* 5 appears to be unable to synthesize GlcNAc, we performed a Delta BLAST search of its genome (26) for homologs of *E. coli* enzymes involved in PG biosynthetic pathways. As shown in Fig. 2A, we could identify genes encoding all the PG biosynthetic enzymes except for three: GlmS, GlmU, and GlmM, which convert fructose-6-P into UDP-*N*-acetylglucosamine (UDP-GlcNAc). GlmS is a glucosamine-6-P-synthase responsible for the conversion of fructose-6-P into glucosamine-6-P; GlmM is a phosphoglucosamine mutase that converts glucosamine-6-P into glucosamine-1-P; GlmU is a bifunctional enzyme, with a C-terminal glucosamine-1-P–*N*-acetyltransferase domain that converts glucosamine-1-P into *N*-acetylglucosamine-1-P and an N-terminal *N*-acetylglucosamine-1-P uridyltransferase domain that converts GlcNAc-1-P into UDP-GlcNAc (27). Since the lack of any of these enzymatic activities is lethal in *E. coli* (27), we assumed that it is the lack of these enzymes that makes *C. canimorsus* dependent on exogenous GlcNAc for growth. If this hypothesis were correct, expression of these three enzymes in *PUL5* mutant bacteria would enable them to synthesize GlcNAc and restore growth and bacterial shape in coculture with HEK293 cells. We cloned the three *E. coli* glm genes alone and in combination in a *C. canimorsus* expression vector (23) and monitored the growth and morphology of recombinant *PUL5* mutants in coculture with HEK293 cells. *PUL5*-deficient bacteria expressing both GlmU and GlmM grew to the same extent as wt and showed a normal shape, indicating that these enzymatic activities allow *C. canimorsus* to synthesize GlcNAc (Fig. 2C and D).

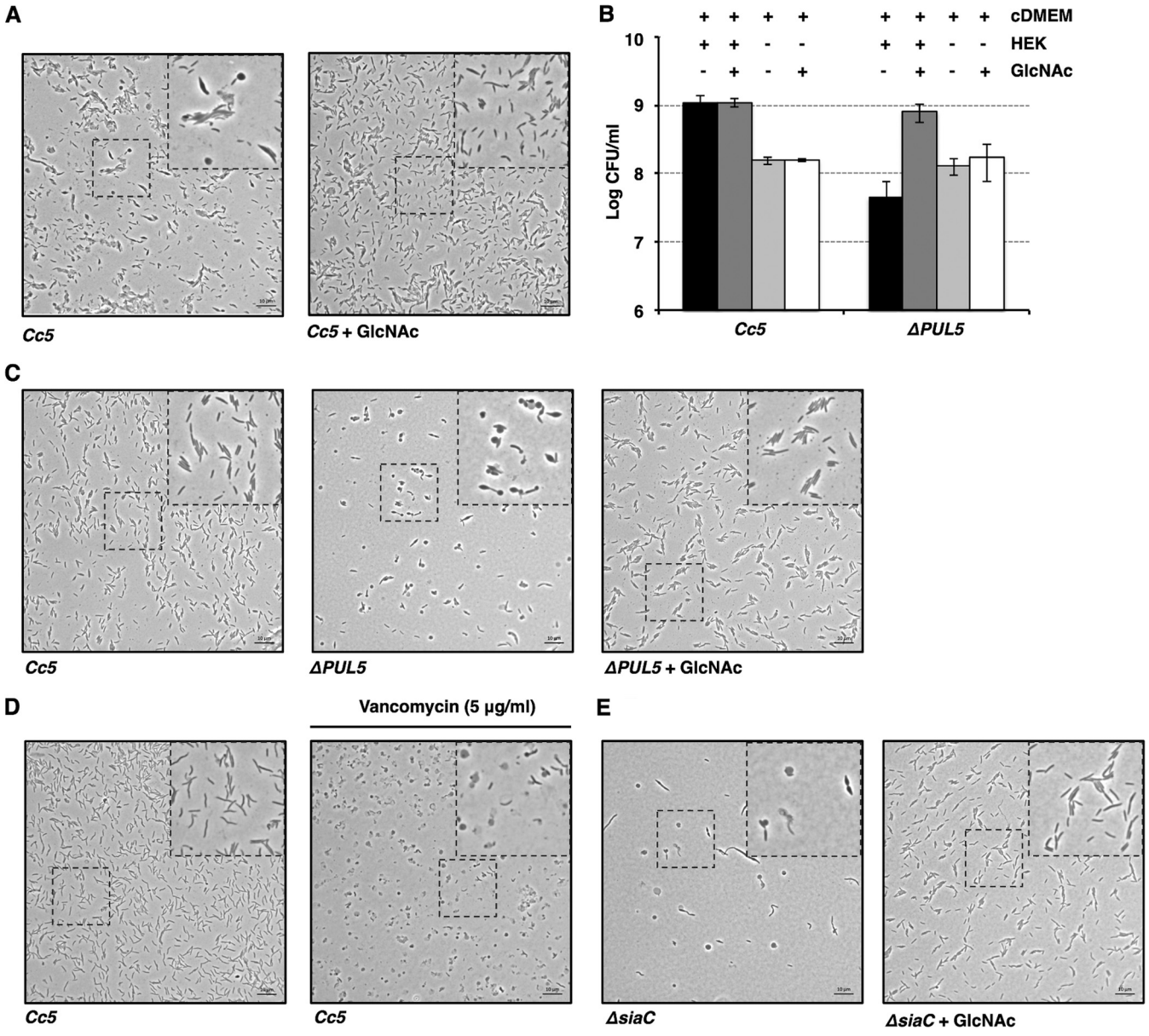

FIG 1 *N*-acetylglucosamine starvation affects growth and cell shape. (A) Bright-field microscopy pictures of wt (*C. canimorsus* 5) bacteria grown for 48 hours on blood agar plates in the absence or in the presence of GlcNAc (0.005%). (B) Counts of wt (*C. canimorsus* 5) and *PUL5* (Δ*PUL5*) knockout bacteria after 23 hours growth in cDMEM with or without HEK293 cells (MOI, 0.05) and in the presence or in the absence of GlcNAc (0.005%). The averages from three independent experiments are shown. Error bars represent 1 standard deviation from the mean. See also Fig. S1A in the supplemental material. HEK293 cells provided GlcNAc captured by the *PUL5*-encoded Gpd complex. Note that HEK293 cells provided more than GlcNAc to wt *C. canimorsus* 5. (C) Bright-field microscopy pictures of wt (*C. canimorsus* 5) and *PUL5* (Δ*PUL5*) bacteria after 23 hours growth on HEK293 cells. See also Fig. S1B. (D) Bright-field microscopy pictures of wt (*C. canimorsus* 5) bacteria grown on HEK293 cells for 12 hours and an additional 4 hours with or without vancomycin (5 μg/ml). See also Movies S1 and S2 in the supplemental material. (E) Bright-field microscopy pictures of sialidase mutant bacteria (Δ*siaC*) grown for 23 hours on HEK293 cells (MOI, 0.05) in the absence or in the presence of GlcNAc (0.005%).

The fact that the expression of GlmM and GlmU alone was sufficient to make *PUL5* mutant bacteria independent of GlcNAc suggested that the *C. canimorsus* 5 genome encodes a glucosamine synthase (GlmS) that was not identified by our BLAST search. Furthermore, since the addition of GlcNAc to the coculture of HEK293 cells completely restored the growth of *PUL5* mutant bacteria, we inferred that *C. canimorsus* is able to synthesize UDP-GlcNAc from GlcNAc, implying that a *C. canimorsus* 5 gene encodes a GlcNAc-1-P uridyltransferase. If this is correct, the phosphoglucosamine mutase GlmM and only the glucosamine-1-P−*N*-acetyltransferase domain of GlmU would be sufficient to compensate for the *PUL5* deletion. To test this hypothesis, we generated two truncated GlmU protein variants: one with the first 77 residues deleted (GlmU del78), consisting only of the glucosamine-1-P−*N*-acetyltransferase activity, and one with the last 125 residues deleted (GlmU Tr331), consisting only of the *N*-acetylglucosamine-1-P-uridyltransferase activity (28) (Fig. 2B). We expressed in *PUL5* mutants either GlmM and GlmU del78 or GlmM and GlmU

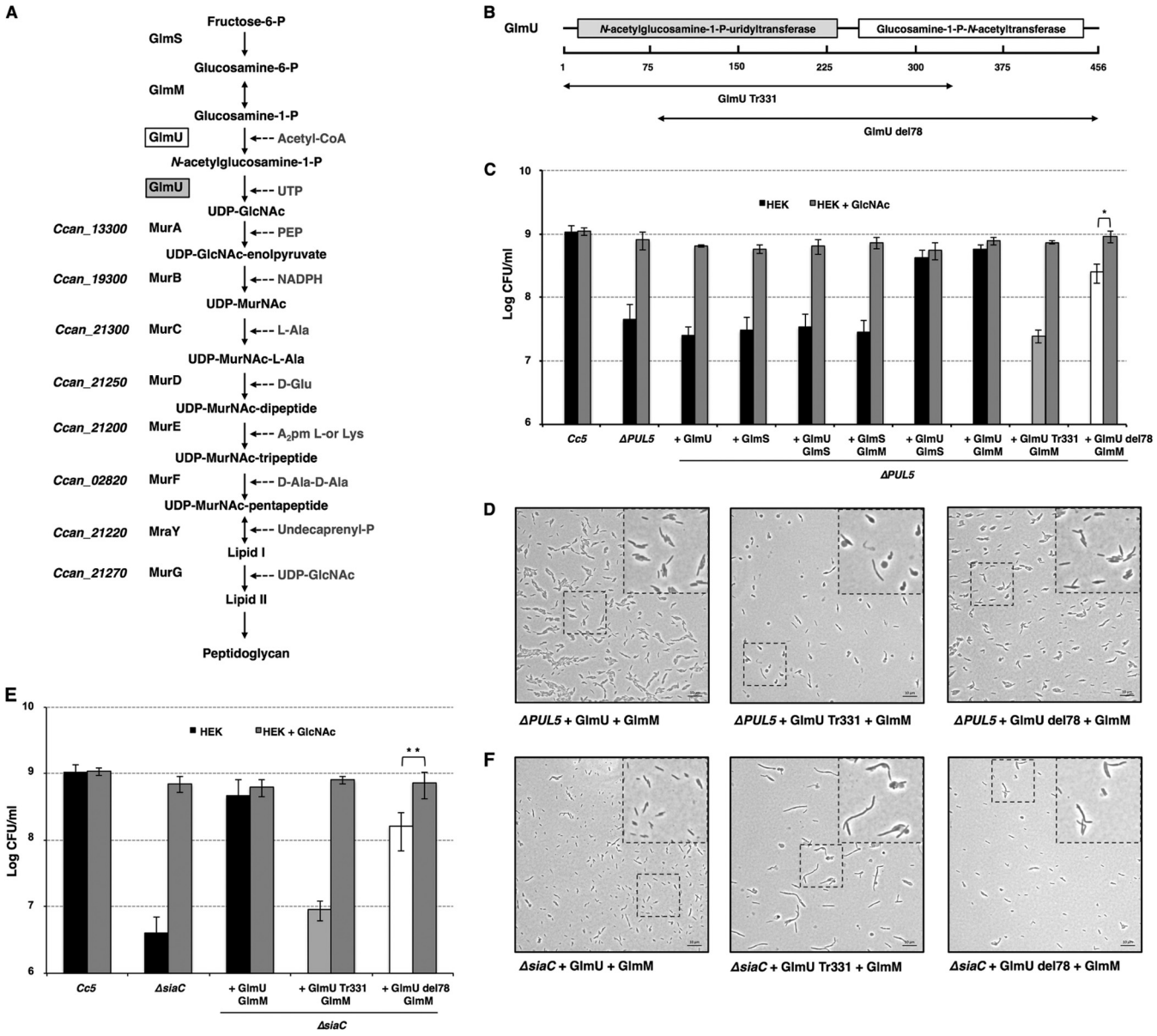

FIG 2 Heterologous expression of GlmU and GlmM in *PUL5* and *siaC* mutant bacteria restores growth and normal cell shape. (A) Peptidoglycan biosynthetic pathway showing *C. canimorsus* 5 orthologs of the *E. coli* enzymes. (B) Schematic representation of the *E. coli* GlmU bifunctional protein. The protein domains are boxed. The recombinant monofunctional proteins are indicated by the arrows. (C) Growth in coculture with HEK293 cells of *PUL5* (Δ*PUL5*) mutant bacteria producing different combinations of GlmS, GlmM, GlmU, and monofunctional GlmU (MOI, 0.05; 23 h of growth). The averages from three independent experiments are shown. Error bars represent 1 standard deviation from the mean. *, $P < 0.05$. (D) Bright-field microscopy pictures of bacteria grown for 23 h with HEK293 cells (MOI, 0.05). (E) Growth on HEK293 cells of of wt (*C. canimorsus* 5) and *siaC* (Δ*siaC*) bacteria expressing GlmM and monofunctional GlmU (MOI, 0.05; 23 h of growth). The averages from three independent experiments are shown. Error bars represent 1 standard deviation from the mean. **, $P < 0.01$. (F) Bright-field microscopy pictures of bacteria grown for 23 h on HEK293 cells (MOI, 0.05).

Tr331, and we monitored the growth and bacterial shapes in coculture with HEK293 cells. As shown in Fig. 2C and D, the expression of GlmM and the GlmU glucosamine-1-P–*N*-acetyltransferase domain (GlmU del78) was sufficient to allow *PUL5* mutant bacteria to behave similarly to wt. Expression of GlmM and the uridyltransferase domain of GlmU (GlmU Tr331) restored neither the growth nor the bacterial shape of *PUL5* mutants (Fig. 2C and D). Quite expectedly, the expression of GlmM and GmU del78 had the same rescuing effect on *siaC* mutants (Fig. 2E and F). The slight but significant differences between the growth and the cell shape observed in *PUL5* and *siaC* mutants expressing GlmM and GlmU del78 and the wt could be ascribed to the reduced enzymatic activity of GlmU del78 compared to the full-length GlmU, as already described by Pompeo and colleagues (28).

Taken together, these results indicate that the inability of *C. canimorsus* 5 to synthesize GlcNAc is due to the lack of two enzymes, a phosphoglucosamine mutase and a glucosamine-1-P–*N*-acetyltransferase.

***C. canimorsus* 5 encodes a new *N*-acetylglucosamine-1-P-uridyltransferase.** In order to identify the unknown *N*-acetyl-

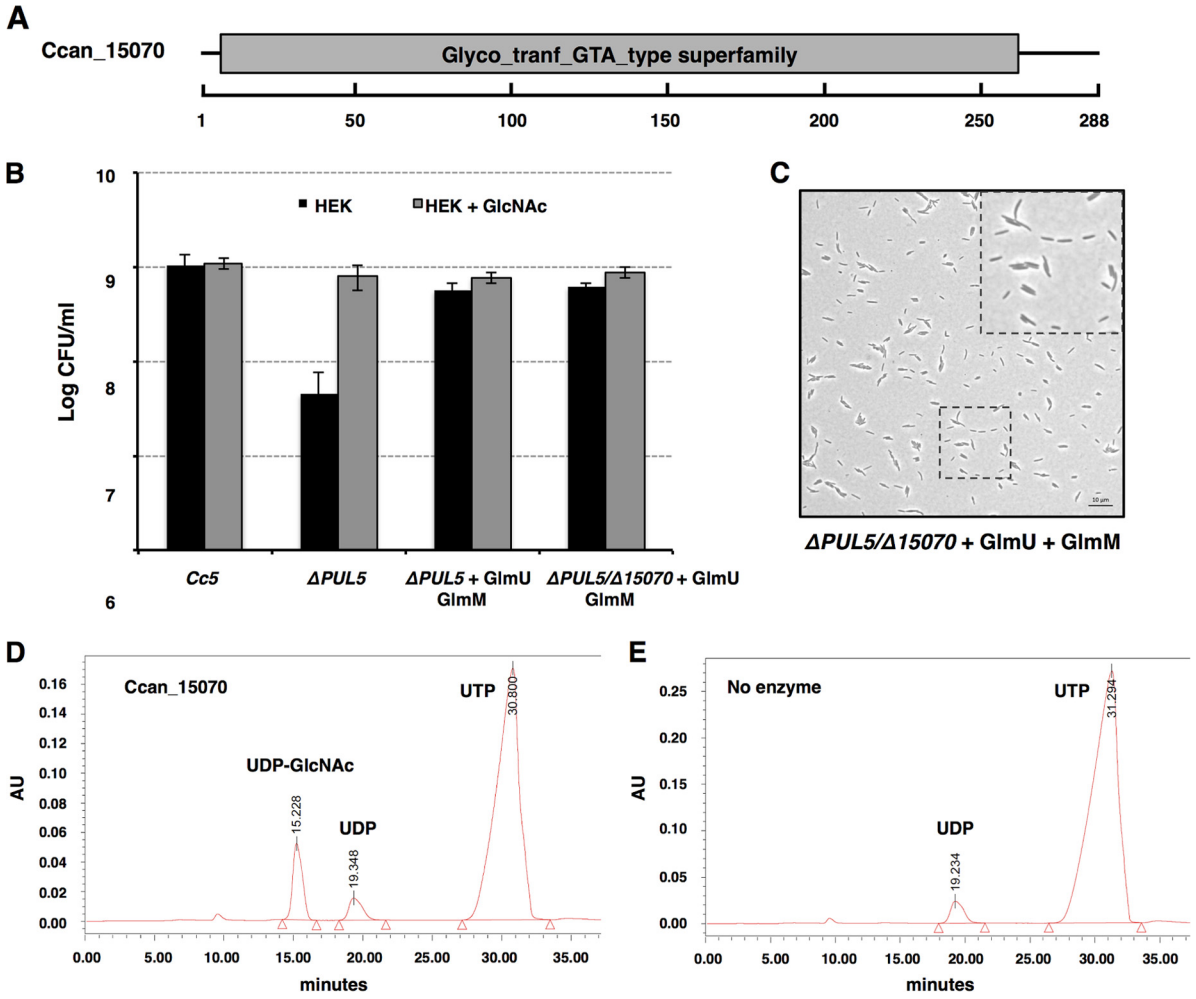

FIG 3 Ccan_15070 encodes an *N*-acetylglucosamine-1-P uridyltransferase. (A) Schematic representation of the *C. canimorsus* 5 *Ccan_15070* gene-encoded *N*-acetylglucosamine-1-P-uridyltransferase (Uniprot ID F9Yr13). (B) Growth on HEK293 cells of wt (*C. canimorsus* 5), *PUL5* (Δ*PUL5*), and *PUL5*/Ccan_15070 (Δ*PUL5*/ΔCcan_15070) double-mutant bacteria expressing GlmM and GlmU (MOI, 0.05; 23 h of growth). The averages from three independent experiments are shown. Error bars represent 1 standard deviation from the mean. (C) Bright-field microscopy picture of *PUL5* Ccan_15070 double mutant bacteria expressing GlmM and GlmU grown for 23 h on HEK293 cells (MOI, 0.05). (D) Detection of UDP-GlcNAc production by HPLC. Incubation of recombinant Ccan_15070 with UTP and GlcNAc-1-P resulted in the production of UDP-GlcNAc. (E) No UDP-GlcNAc formation could be detected in the absence of recombinant Ccan_15070.

glucosamine-1-P-uridyltransferase of *C. canimorsus* 5, we searched the genome for gene products with an enzymatic domain similar to that of the N-terminal *N*-acetylglucosamine-1-P-uridyltransferase domain of the *E. coli* GlmU. It turned out that Ccan_15070 encodes a protein with a conserved glycosyltransferase domain (Fig. 3A). Attempts to knock out Ccan_15070 were unsuccessful unless *C. canimorsus* 5 could synthesize the *E. coli* GlmU Tr331 protein, suggesting that Ccan_15070 is an essential gene and indeed encodes an *N*-acetylglucosamine-1-P-uridyltransferase.

We then generated a *PUL5* Ccan_15070 double-knockout strain complemented with the *E. coli glmM* and *glmU* genes and monitored growth and cell morphology. As shown in Fig. 3B and C, the strain grew to the same extent as wt and had a normal cell shape, indicating that the deletion of Ccan_15070 could be fully complemented by the *N*-acetylglucosamine-1-P-uridyltransferase activity of the *E. coli* GlmU.

Finally, to test the Ccan_15070 enzymatic activity, we expressed the protein with a C-terminal Strep tag in *E. coli* and we added purified Ccan_15070 to a solution of GlcNAc-1-P and UTP. The analysis of the reaction products via high-performance liquid chromatography (HPLC) confirmed the production of UDP-GlcNAc (Fig. 3D). Thus, Ccan_15070 encodes an *N*-acetylglucosamine-1-P-uridyltransferase, which we named $GlmU_{Cc}$.

GlcNAc is also harvested through a PUL-encoded system targeting mucin. The loss of the capacity to synthesize aminosugars during evolution implies that *C. canimorsus* relies on aminosugars from the dog mouth. In the oral cavity, one of the most abundant glycoproteins is mucin, which is heavily glycosylated and harbors mainly O-linked glycans. The *PUL5*-encoded Gpd system can thus not harvest the mucin sugars. In order to determine if the aminosugars from mucin O-glycans can be used to synthesize PG, we took advantage of the fact that *PUL5* mutant bacteria grow less well than wt in coculture with HEK293 cells. Hence, we tested whether the addition of purified bovine submaxillary mucin restored the growth of *PUL5* bacteria. As shown in Fig. 4G and H,

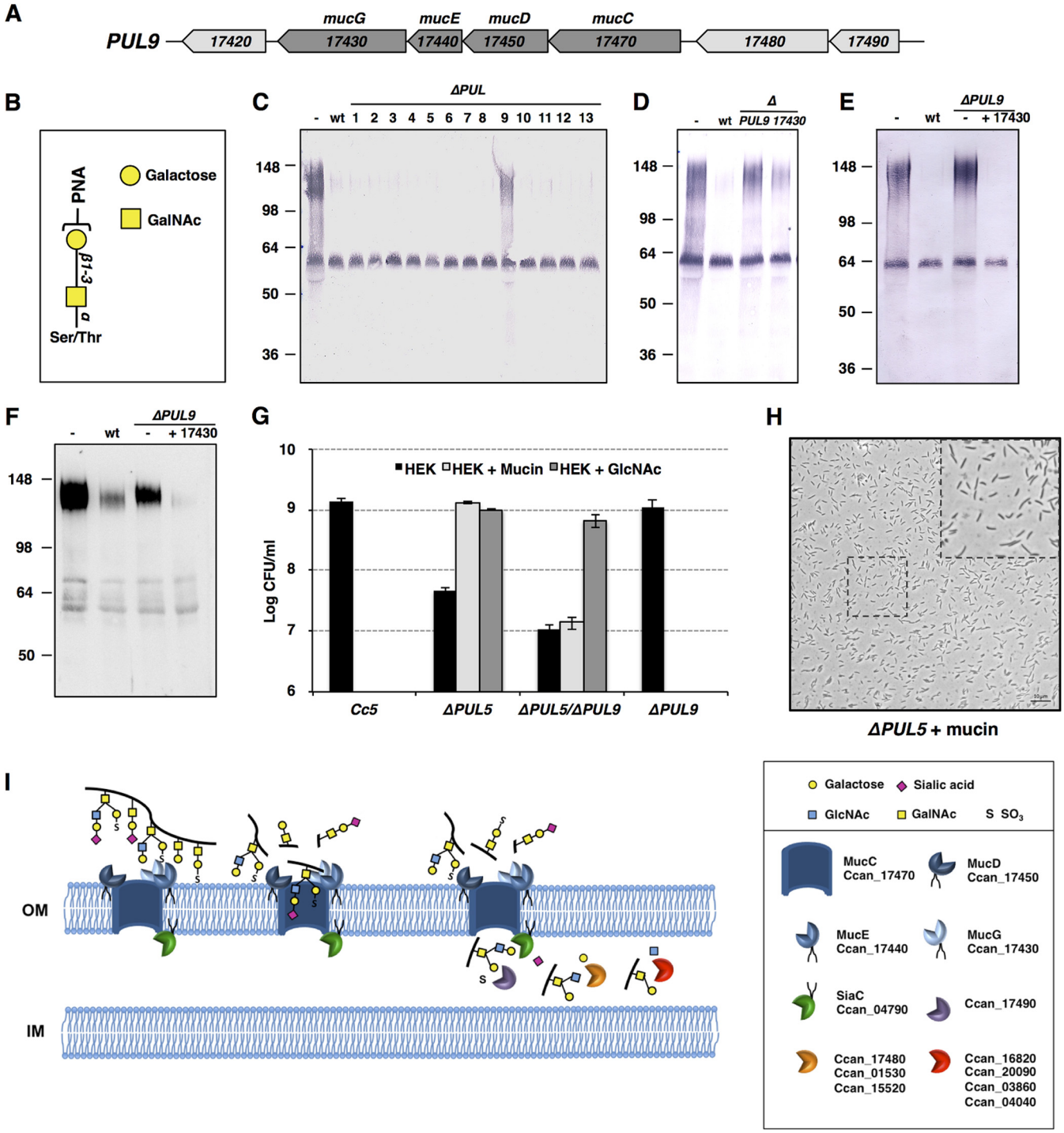

FIG 4 *PUL9* gene products allow mucin degradation and deglycosylation. (A) Schematic representation of the *PUL9* locus. (B) Schematic drawing of the PNA lectin target oligosaccharides. (C) PNA lectin staining of human saliva after incubation in the presence of wt *C. canimorsus* 5 and the 13 *PUL* knockout strains. The upper band represents mucin, while the lower band represents sIgA. (D) Saliva PNA staining after incubation with wt bacteria, *PUL9*, and Ccan_17430 knockout bacteria. (E) Saliva PNA staining after incubation with wt bacteria, *PUL9*, or *PUL9* bacteria expressing the only Ccan_17430 protein. (F) Western blot analysis of human mucin 7 in saliva after incubation with wt bacteria, *PUL9*, or *PUL9* bacteria expressing the only Ccan_17430 protein. See also Fig. S3 in the supplemental material. (G) Growth after 23 h of wt (*C. canimorsus* 5), *PUL5* (Δ*PUL5*), *PUL9* (Δ*PUL9*), and *PUL5/PUL9* (Δ*PUL5* Δ*PUL9*) mutant bacteria in the presence of HEK293 cells with or without bovine submaxillary gland mucin (1 mg/ml) or GlcNAc (0.005%) (MOI, 0.005). The averages from three independent experiments are shown. Error bars represent 1 standard deviation from the mean. (H) Bright-field microscopy picture of *PUL5* (Δ*PUL5*) mutant bacteria grown for 23 h on HEK293 cells in the presence of bovine mucin (1 mg/ml) (MOI, 0.05). (I) Functional model of mucin degradation and deglycosylation. Mucin is bound at the bacterial surface by the MucCDEG surface protein complex. The MucG protease cleaves mucin into glycosylated peptides that are imported into the periplasm through the MucC pore. Terminal sialic acid is cleaved by sialidase (SiaC), and terminal sulfate groups are removed by the sulfatase. The glycan is further processed by the sequential activity of several periplasmic exoglycosidases that allow the liberation of monosaccharides.

addition of bovine mucin fully restored the growth and the morphology of *PUL5* mutant bacteria.

To ascertain that salivary mucins are deglycosylated by *C. canimorsus* 5, we incubated bacteria with filtered fresh human saliva and we analyzed the salivary glycoproteins before and after incubation, by using sodium dodecyl sulfate-polyacrylamide gel electrophoresis followed by staining with peanut agglutinin (PNA). PNA recognizes terminal galactose linked to GalNAc in O-linked oligosaccharides, a glycan structure named T-antigen (Fig. 4B) that is abundant in mucins (29). A saliva glycoprotein with a molecular mass around 100 to 140 kDa turned out to be deglycosylated after incubation with wt *C. canimorsus* 5 (Fig. 4C). In contrast, the glycosylation state of a protein with a molecular mass of around 60 kDa was unaffected (Fig. 4C). LC-mass spectrometry (LC/MS) analysis of the two proteins identified the higher-molecular-mass protein as salivary mucin (MUC7 or MG2; Uniprot accession number Q8tax7) and the lower-molecular-mass one as secreted IgA (sIgA, or Ig α-1 chain region; Uniprot accession number P01876) (data not shown). This indicated that *C. canimorsus* 5 specifically targeted MG2 glycans rather than the sIgA ones. We reasoned that one of the 13 *PUL* mutants could be responsible for the T-antigen cleavage from MG2, and we tested the 13 *C. canimorsus* 5 *PUL* knockout mutants (15). Of all the *PUL* mutants, only *PUL9* knockout bacteria were impaired in MG2 T-antigen deglycosylation (Fig. 4C). To ensure that mucin utilization was *PUL9* dependent, we generated a *PUL5 PUL9* double-knockout strain and tested whether addition of mucin restored the growth of this mutant. As expected, addition of mucin did not restore the growth defect of the double mutant, indicating that mucin degradation and utilization are *PUL9* dependent (Fig. 4G).

***PUL9* encodes a bona fide Sus-like complex.** *PUL9* encodes seven proteins (Ccan_17420 to Ccan_17490) (Fig. 4A). The neighboring Ccan_17470 and Ccan_17450 genes encode typical SusC-like (TonB-dependent receptor) and SusD-like proteins. Ccan_17480 is annotated as a β-galactosidase, while Ccan_17490 is a putative sulfatase. Both carry a signal peptide I and hence are predicted to be periplasmic. Ccan_17420 is a predicted lipoprotein annotated as a carboxypeptidase. Ccan_17430 is predicted to be a mucinase (30) with two BACON (*Bacteroidetes*-associated carbohydrate often N-terminal domain) modules (31) and one F5/8 type C (32) carbohydrate binding module. Ccan_17440 is the most abundant *PUL*-encoded protein of the *C. canimorsus* 5 surfome (15) and also harbors an F5/8 type C carbohydrate binding module. Ccan_17430 (mucinase) and Ccan_17450 (SusD-like) were also found in the surfome of *C. canimorsus* 5 (15). In order to determine whether all these proteins form with Ccan_17470 (SusC-like), a surface complex similar to the one formed by the *PUL5* products, we tagged the C terminus of the porin Ccan_17470 and carried out a His-Strep tandem affinity purification (see Fig. S2 in the supplemental material). The LC/MS analysis of the eluate identified 35 proteins (see Table S1 in the supplemental material), among which were Ccan_17450, Ccan_17440, and Ccan_17430. Thirteen proteins were identified in the mock eluate, of which 11 were also present in the Ccan_17470–Strep-His eluate. No *PUL9*-encoded product was identified in the mock eluate (see Table S1). These data suggest that Ccan_17470, Ccan_17450, Ccan_17440, and Ccan_17430 form a complex at the bacterial surface. Hence, *PUL9* encodes a bona fide Sus-like complex, and we propose to call MucC the SusC-like protein, MucD the SusD-like protein, MucG the putative mucinase, and MucE the four surface proteins (Fig. 4A). Interestingly, among the proteins that eluted with the Muc complex, we also identified a sialidase. This periplasmic enzyme was previously found to be associated with the Gpd complex and involved in N-glycan processing (22). Thus, we could also envision involvement of this protein in mucin glycan processing.

The hydrolytic enzyme from the complex is not a glycan hydrolase but a mucin peptidase. As already mentioned, Ccan_17430 is predicted to be a mucinase (30) with two BACON (31) and one F5/8 type C (32) carbohydrate binding modules.

Since *PUL*-encoded complexes are usually devoted to the hydrolysis of complex carbohydrates (33), the presence of a protein hydrolase was unexpected. In order to verify the function of Ccan_17430, we incubated human saliva with wt and Ccan_17430 mutant bacteria and monitored mucin glycosylation via PNA staining. Deletion of Ccan_17430 abolished mucin deglycosylation (Fig. 4D). Furthermore, expression of Ccan_17430 in a *PUL9* deletion background led to a complete loss of mucin staining by PNA, suggesting that Ccan_17430 alone is responsible for the observed phenotype (Fig. 4E). We then monitored the presence of mucin MG2 by Western blotting and found that it was dramatically decreased, indicating that Ccan_17430 indeed encodes a protease that cleaves mucin (Fig. 4F). In agreement with this, purified recombinant Ccan_17430 fully degraded MG2 from human saliva (see Fig. S3 in the supplemental material). Addition of EDTA completely blocked the mucinase activity, indicating that Ccan_17430 is a metallopeptidase. Removal of the N-terminal conserved BACON and F5_F8 type C glycan binding domains led to reduced mucin degradation activity, suggesting that these domains could play a role in mucin binding, even though the truncated protein was still able to bind and degrade MG2.

Thus, the *PUL9*-encoded system appears to be quite different from the canonical ones, such as the Sus (33) and Gpd (22) systems, where a glycosylhydrolase at the bacterial surface is responsible for the cleavage of complex sugars like starch or N-linked glycans. In the case of *PUL9*, it is a protease that attacks mucin at the bacterial surface, generating glycosylated peptides.

DISCUSSION

Here, we addressed the question of the phenotypic polymorphism of *C. canimorsus* (1), and we found that it is linked to the adaptation of *C. canimorsus* to its host. We showed that *C. canimorsus* does not undergo a kind of phase variation but, instead, endures aminosugar starvation, which leads to bacterial growth arrest and cell shape change. This phenotype is a consequence of the blockade of peptidoglycan synthesis. These findings are explained by the fact that *C. canimorsus* relies on exogenous aminosugars because it is unable to synthesize its own GlcNAc. Bacteria generally synthesize GlcNAc starting from fructose-6-P through a series of metabolic steps (Fig. 2A). *In silico* analysis of the genome of *C. canimorsus* 5 did not identify orthologs of all the necessary genes. Furthermore, coexpression of the *E. coli* GlmM and the GlmU glucosamine-1-P–*N*-acetyltransferase domain completely restored the growth and cell morphology of *PUL5* mutant bacteria. We conclude from these results that *C. canimorsus* is unable to synthesize GlcNAc because of the lack of these two enzymatic activities. Furthermore, we identified and characterized a novel *N*-acetylglucosamine-1-P-uridyltransferase that is able to synthesize UDP-GlcNAc from GlcNAc-1-P. Differently from *E. coli* and other well-studied bacteria, where the glucosamine-

1-P−*N*-acetyltransferase and the *N*-acetylglucosamine-1-P-uridyltransferase activities are found in the same protein (GlmU) (27), the *C. canimorsus* enzyme ($GlmU_{Cc}$) is monofunctional, harboring only the *N*-acetylglucosamine-1-P-uridyltransferase activity and missing the glucosamine-1-P−*N*-acetyltransferase one.

We reasoned that the loss of capacity to synthesize GlcNAc could be a common feature in the phylum *Bacteroidetes*. We performed an *in silico* search for orthologs of $GlmU_{Cc}$ in bacteria and found that, indeed, in *Bacteroidetes*, 30 out of 45 genera have a monofunctional ortholog of $GlmU_{Cc}$ (see Fig. S4 in the supplemental material). This suggests that, like *C. canimorsus* 5, most *Bacteroidetes* are unable to synthesize GlcNAc and so rely on exogenous aminosugars.

The loss of the capacity to synthesize *N*-acetylated aminosugars during evolution implies that *C. canimorsus* relies on aminosugars from its ecological niche, the dog mouth. In agreement with this hypothesis, we showed that *C. canimorsus* 5 degrades salivary mucin, a protein that is heavily O-glycosylated and very abundant in saliva. Mucin degradation was found to depend on a mucin protease (MucG), which is, unexpectedly, part of a Sus-like surface complex encoded by the *PUL9* locus. Nevertheless, mucin degradation rescued the growth of a *PUL5* mutant, indicating that mucin aminosugars can be taken up and metabolized. Given the structure of mucin, a protease is probably as efficient as a glycosyl hydrolase in liberating carbohydrates. This is nevertheless the first example of a *PUL*-encoded complex endowed with a protease activity. It is also the first example of an oral commensal that utilizes mucin via a *PUL*-encoded system. The *C. canimorsus* 5 *PUL9* shows high similarity in gene composition and organization to the *Bacteroides thetaiotaomicron* BT4240-50 *PUL*, which is induced by the presence of mucin O-glycans (16). Like *PUL9*, besides the SusC and SusD-like proteins, the BT4240-50 *PUL* encodes a mucinase (BT4244) that has been shown to target bovine mucin *in vitro* (30). However, the *C. canimorsus* 5 and BT mucinases share only 27% identity. Both loci encode periplasmic β-galactosidases (Ccan_17480 and BT4241) that are 34% identical and likely to be involved in mucin glycan processing. In *B. thetaiotaomicron*, the β-galactosidase has been found to be constitutively expressed (16). *PUL9* also encodes a putative periplasmic sulfatase (Ccan_17490), which is similar (47% identity) to the mucin-desulfating sulfatase BT3177 (34). We reason that these two enzymes could act on mucin glycans once the glycosylated peptides are transferred into the periplasm through the Ccan_17470 MucC pore. Mucin O-glycans are mainly composed of core 1- and core 2-type *O*-glycans that can harbor terminal sulfate groups (SO_3) and sialic acid residues (29). One can thus envision a mucin degradation and deglycosylation model where mucin is first bound at the bacterial surface by the MucCDGE surface complex, then cleaved by the activity of the MucG mucinase, which liberates glycosylated peptides that are translocated into the periplasm through the MucC pore. Once in the periplasm, the glycopeptides are subsequently processed by periplasmic enzymes; the removal of terminal sialic acid residues by sialidase (Ccan_04780) and of terminal sulfate groups by the Ccan_17490 sulfatase make galactose accessible to β-galactosidases (Ccan_17480, Ccan_01530, and Ccan_15520) whose activities allow the β-*N*-acetylglucosaminidases (Ccan_16820, Ccan_20090, Ccan_03860, and Ccan_04040) to liberate the GlcNAc residues present in core 2-type O-glycans (Fig. 4I). The *PUL9* locus also encodes, downstream from MucG, a putative lipoprotein with a carboxypeptidase domain (Ccan_17420) (Fig. 4A). The presence of this enzyme in the locus suggests an involvement in the processing of mucin glycopeptides once in the periplasm, but this was not investigated. Our data thus characterize a novel *PUL*-encoded system which allows harvesting of mucin glycan by the activity of a mucinase at the bacterial surface.

Overall, this work illustrates how a commensal that has evolved to adapt to a specific niche becomes dependent on that niche. *C. canimorsus* adapted to the dog mouth by acquiring or evolving two Sus-like machines that are tuned to harvest sugars from saliva and possibly from the oral epithelium. Since these machines provide abundant aminosugars, *C. canimorsus* could lose the capacity to synthesize GlcNAc. Interestingly, *C. canimorsus* has two Sus-like machines, allowing it to retrieve aminosugars. One of these, the Muc machine, can only be of use in the mouth, but the other one, the Gpd machine, is able to sustain growth in other compartments of a host and probably represents a virulence factor (15, 21).

Recently, it was shown that several members of the genus *Bacteroides*, which are able to utilize different polysaccharides, liberate polysaccharide breakdown products that can be consumed by bacteria from other species unable to grow on the polysaccharide alone (35). These findings indicate that, in the human gut microbial ecosystem, there are syntrophic interactions between different bacteria. Similar syntrophic interactions might well occur in the dog mouth, since the biology of *C. canimorsus* resembles that of *B. thetaiotaomicron*, but the dog oral ecosystem is quite different from the intestine in the sense that digestion does not start in the dog mouth and hence the microbial competition may be more fierce. In addition, *PUL5*-deficient *C. canimorsus* cannot be cross-fed by wt *C. canimorsus* (21), which can be explained by the mechanisms of uptake and processing of host glycans by the Gpd apparatus where N-glycans are cleaved and likely immediately imported into the periplasm (22). It is likely that the same applies to the Muc apparatus, but this was not investigated. For *C. canimorsus*, we can thus envision a scenario that is different from the one of the human gut. *Capnocytophaga* could have a more "selfish" behavior, as it harvests, takes up, and utilizes its own glycans, avoiding release of polysaccharide breakdown products, which could be utilized by competitor bacteria.

MATERIALS AND METHODS

Bacterial strains and growth conditions. (i) Conventional bacterial growth conditions and selective agents. The strains used in this study are listed in Table S2 in the supplemental material. *Escherichia coli* strains were routinely grown in LB broth at 37°C. *C. canimorsus* bacteria were routinely grown on heart infusion agar (HIA; Difco) supplemented with 5% sheep blood (Oxoid) for 2 days at 37°C in the presence of 5% CO_2. To select for plasmids, antibiotics were added at the following concentrations: 10 μg/ml erythromycin (Em), 10 μg/ml cefoxitin (Cf), 20 μg/ml gentamicin (Gm), 100 μg/ml ampicillin (Ap), 50 μg/ml kanamycin (Km), and 10 μg/ml tetracycline (Tc). GlcNAc (catalog number A8625; Sigma) was added at a final concentration of 0.005% when indicated.

(ii) Growth of *C. canimorsus* 5 bacteria with HEK293 cultured cells. HEK293 cells were cultured in Dulbecco's modified Eagle's medium (DMEM; Invitrogen) with 10% (vol/vol) fetal calf serum (Invitrogen) and 1 mM sodium pyruvate (cDMEM). Cells were grown in medium without antibiotics in a humidified atmosphere enriched with 5% CO_2 at 37°C. Bacteria were harvested by gently scraping colonies off the agar surface and resuspended in phosphate-buffered saline (PBS). A total of 1×10^4 bacteria were incubated with 2×10^5 HEK293 cells (multiplicity of infection [MOI], 0.05) in a final volume of 1 ml medium devoid of antibiotics for 23 h.

(iii) Monitoring bacterial growth in HEK293 cell cultures. A total of 1×10^4 bacteria were added to 2×10^5 HEK293 cells (MOI, 0.05) in a final volume of 1 ml medium devoid of antibiotics. At different times, the medium containing bacteria and cells was collected and serially diluted. Dilutions were plated on HIA 5% sheep blood plates. After 48 h of incubation at 37°C with 5% CO_2, bacterial colonies were counted.

(iv) Growth in HEK293 cell cultures in the presence of bovine mucin. A total of 1×10^4 bacteria were incubated with 2×10^5 HEK293 cells (MOI, 0.05) in a final volume of 1 ml medium devoid of antibiotics and with 1 mg of mucin from bovine submaxillary glands (catalog number M3895; Sigma-Aldrich).

Mutagenesis and allelic exchange. Mutagenesis of *C. canimorsus* 5 wt was performed as described in reference 36 with slight modifications. The oligonucleotides used in this study are listed in Table S4 in the supplemental material. Briefly, replacement cassettes with flanking regions spanning approximately 500 bp homologous to the direct target gene-framing region were constructed with a three-fragment overlapping-PCR strategy. First, two PCRs were performed on 100 ng of *C. canimorsus* 5 genomic DNA with primers A and B for the upstream flanking regions and with primers C and D for the downstream regions. Primers B and C contained an additional 5′ 20-nucleotide extension homologous to the resistance *erm*(F) insertion cassette or to the *tet*(Q) insertion cassette. The *erm*(F) resistance cassette was amplified from plasmid pmm106 DNA (36) with primers 5502 and 5503. The *tet*(Q) resistance cassette was amplified from plasmid pfl38 DNA (see Table S3 in the supplemental material) with primers 7180 and 7181. All three PCR products were cleaned and then mixed in equal amounts for PCR using Phusion polymerase (Finnzymes). The initial denaturation was at 98°C for 2 min, followed by 12 cycles without primers to allow annealing and then elongation of the overlapping fragments (98°C for 30 s, 50°C for 40 s, and 72°C for 2 min). After the addition of external primers (A and D), the program was continued with 20 cycles (98°C for 30 s, 50°C for 40 s, and 72°C for 2 min 30 s) and finally 10 min at 72°C. Final PCR products consisted of the target gene with *erm*(F) or *tet*(Q) insertion cassettes and were then digested with PstI and SpeI for cloning into the appropriate sites of the *C. canimorsus* suicide vector pMM25 (36). Resulting plasmids were transferred by RP4-mediated conjugative DNA transfer from *E. coli* S17-1 to *C. canimorsus* 5 to allow integration of the insertion cassette. Transconjugants were then selected for the presence of the *erm*(F) or *tet*(Q) cassettes on erythromycin or tetracycline plates, respectively, and then checked for sensitivity to cefoxitin. Correct cassette insertions were confirmed by sequencing.

Construction of complementation and expression plasmids. Plasmids and oligonucleotides used in this study are listed in Tables S3 and S4 in the supplemental material.

(i) Construction of GlmM-, GlmU-, and GlmS-expressing vectors. Full-length *glmS* and *glmU* were amplified from *E. coli* MG1655 DNA with primers 7412/7413 and 7406/7407, respectively, and cloned into plasmid pPM5 (23) into *NcoI* and *XhoI* restriction sites, leading to plasmids pFR11 and pFR12. Full-length *glmU* and *glmS* were coamplified from *E. coli* MG1655 DNA by using primers 7406 and 7413 and cloned into pPM5 by using *NcoI* and *XhoI* restriction sites, leading to plasmid pFR13. Full-length *E. coli* glmM was amplified from *E. coli* MG1655 DNA with primers 7415 and 7416 and cloned downstream of the *glmS* gene into pFR11 by using *XhoI* and *SpeI* restriction sites, leading to plasmid pFR14. Full-length *E. coli* glmM was amplified from *E. coli* MG1655 DNA with primers 7415 and 7416 and cloned downstream of the *glmS* gene into pFR13 by using *XhoI* and *SpeI* restriction sites, leading to plasmid pFR15. Full-length *E. coli glmM* was amplified from *E. coli* MG1655 DNA with primers 7415 and 7416 and cloned downstream of the *glmU* gene into pFR12 by using *XhoI* and *SpeI* restriction sites, leading to plasmid pFR16. *E. coli* glmU with the first 77 codons deleted (GlmU del78) was amplified with primers 7422 and 7407 and cloned into pFR16 by using *NcoI* and *XhoI* restriction sites, leading to plasmid pFR17. *E. coli glmU* with codons 332 to 456 deleted (GlmU Tr331) was amplified from *E. coli* MG1655 DNA with primers 7406 and 7421 and cloned into pFR16 by using *NcoI* and *XhoI* restriction sites, leading to plasmid pFR18.

(ii) Construction of $GlmU_{Cc}$- and MucG-overexpressing vectors. To generate $GlmU_{Cc}$ with a C-terminal Strep tag, the $glmU_{Cc}$ gene (Ccan_15070) was amplified with primers 7442 and 7450 and cloned into pET22B(+) by using *NcoI* and *XhoI* restriction sites, leading to plasmid pFR19.

mucG (Ccan_17430), devoid of the first 21 codons and encoding a C-terminal Strep tag, was amplified with primers 7020 and 7021 and cloned into pET22b(+) by using *NcoI* and *XhoI* restriction sites, leading to plasmid pFR22. *mucG* (Ccan_17430), devoid of the first 355 codons and encoding a C-terminal Strep tag, was amplified with primers 7019 and 7021 and cloned into pET22b(+) by using NcoI and XhoI restriction sites, leading to plasmid pFR23.

(iii) Construction of *mucG* complementation vector. The 340-bp region upstream of the *mucC* (Ccan_17470) starting codon sequence, containing the putative *mucC* promoter, was cloned into pMM47A.1 vector (36) by using *SalI* and *NcoI* restriction sites, leading to plasmid pFR20. Full-length *mucG* (Ccan_17430) was amplified with primers 6923 and 6925 and cloned into pFR20 by using *NcoI* and *XbaI* restriction sites, leading to plasmid pFR21.

(iv) Engineering MucC-Strep-His-D, -E, and -G and MucC, -D, -E, and -G expression vectors. To engineer MucC (Ccan_17470) with a C-terminal Strep tag, the gene *mucC* (Ccan_17470) was amplified with primers 6842 and 6786 and cloned into pFR20 with *NcoI* and *XhoI* restriction sites in frame with the 6× His in the vector, leading to plasmid pFR24.

Full-length *mucD*, *mucE*, and *mucG* (Ccan_17450-30) genes were amplified with primers 6846 and 6845 and cloned into pFR24 downstream from *mucC*-Strep-His by using *SpeI* restriction sites, leading to plasmid pFR26. Full-length *mucC* (Ccan_17470) was amplified with primers 6842 and 6805 and cloned into pFR20 with *NcoI* and *XhoI* restriction sites, leading to plasmid pFR25. Full-length *mucD*, *mucE*, and *mucG* (Ccan_17450-30) were amplified with primers 6846 and 6845 and cloned into pFR25 downstream from *mucC* with *SpeI* restriction sites, leading to plasmid pFR27.

(v) Construction of a TetQ expression vector. The *tet*(Q) gene was amplified from pMM104 (36) DNA with primers 7156 and 7157 and cloned into pPM5 by using *NcoI* and *XbaI* restriction sites, leading to plasmid pFL38.

Microscopy pictures and movies. For each experiment, bacterial suspensions were deposited onto 1% agarose pads. All microscopy images were captured with an Axioscop (Zeiss) microscope with an Orca-Flash 4.0 camera (Hamamatsu) and Zen 2012 software (Zeiss). Images were processed using ImageJ software.

(i) Growth curves of bacteria in cocultures with HEK293 cells. For each time point, 10-μl aliquots of bacterium-cell suspensions were transferred onto a 1% agarose pad made with PBS, and images were captured on the microscope.

(ii) Vancomycin treatment of wt bacteria in cocultures with HEK293 cells. wt bacteria were grown for 12 h in HEK293 cell cultures. Vancomycin hydrochloride was then added at a final concentration of 5 μg/ml. Bacteria were collected after 4 h, 10 μl of the bacterium-cell suspension was transferred onto a 1% agarose pad made with PBS, and images were collected on the microscope.

(iii) Microscopy movies of wt bacteria treated with vancomycin. Bacteria were grown to exponential phase on HEK293 cell cultures for 12 h in 1-ml final volumes and then resuspended. Ten microliters of the bacterium-cell suspension was transferred onto a 1% agarose pad made with DMEM with 10% (vol/vol) heat-inactivated human serum (S1-Liter; EMD Millipore) and vancomycin hydrochloride (Sigma-Aldrich) at a final concentration of 5 μg/ml. Time-lapse movies were generated by imaging the cells every 2 min for 12 h. During all microscopy experiments, the stage was kept at 37°C to allow bacterial growth. Movies were generated from time-lapse images using Zen 2012 software (Zeiss).

(iv) Microscopy movies of *PUL5* mutant bacteria. *PUL5* bacteria were grown to exponential phase in HEK293 cell cultures for 12 h in 1-ml final volumes and then resuspended. Ten microliters of the bacterium-cell suspension was transferred onto a 1% agarose pad made with DMEM with 0.5% (vol/vol) heat-inactivated human serum (S1-Liter; EMD Millipore), a condition we found allowed a few bacterial generations before leading to growth arrest and shape change. Time-lapse movies were generated by imaging the cells every 2 min for 12 h. During all microscopy experiments, the stage was kept at 37°C to allow bacterial growth. Movies were generated from time-lapse images by using Zen 2012 software (Zeiss).

Recombinant Ccan_15070 ($GlmU_{Cc}$) and Ccan_17430 (MucG) overexpression and purification. *E. coli* BL21 bacteria harboring plasmid pFR19, expressing a C-terminal Strep-tagged Ccan_15070, or pFR22, expressing a C-terminal Strep-tagged Ccan_17430 or harboring plasmid pFR23, expressing C-terminal Strep-tagged Ccan_17430 devoid of the BACON and F5/8 type C domains, were inoculated at an optical density at 600 nm (OD_{600}) of 0.05 in 300 ml LB medium with ampicillin and grown for 2 h at 37°C with agitation. To induce protein expression, isopropyl-β-D-thiogalactopyranoside was added to a final concentration of 1 mM, and cells were grown for 2 more hours. Bacteria were collected by centrifugation at 5,000 × *g*, resuspended in PBS, and lysed in a French press. Lysates were centrifuged at 15,000 × *g* for 15 min, and supernatants were collected.

Each supernatant was loaded into a column containing 1 ml of a 50% slurry (0.5 ml CV) Strep-Tactin Superflow resin (catalog number 2-1206-002; IBA). The flowthrough was reloaded into the resin 2 more times. The resin was then washed 4 times with 10 CV of buffer W (100 mM Tris, 150 mM NaCl, 1 mM EDTA; pH 8), and proteins were eluted in 3 steps with 0.5 ml elution buffer (100 mM Tris, 150 mM NaCl, 1 mM EDTA, 2.5 mM desthiobiotin; pH 8). The proteins present in the elution fractions were visualized by Coomassie staining and immunoblotting with mouse anti-Strep tag antibodies (MCA2489P; AbD Serotec).

UDP-GlcNAc synthesis by recombinant Ccan_15070 ($GlmU_{Cc}$). The activity and substrate specificity of the enzyme Ccan_15070 was assessed by incubating 30 μg of purified recombinant Ccan_15070 protein with 1,245 μg of UTP (catalog number U6625; Sigma) and 500 μg of GlcNAc-1-P (A2142; Sigma) in 1 ml 100 mM Tris-HCl (pH 7.5) and 10 mM $MgCl_2$ solution for 16 h at 37°C. As a control, the same amount of substrate was incubated in the absence of recombinant purified Ccan_15070. UDP-GlcNAc production was detected by HPLC using a Waters 600 E device with a C_{18} Atlantis T3, 5 μm, 4.60- by 250-mm column. Elution was done with 50 mM triethylimine acetic acid, pH 6.8, 0.5% CH_3CN; detection was at 262 nm and at a flow rate of 1 ml/min.

Human salivary mucin deglycosylation and degradation analyses. Fresh human saliva was collected from healthy volunteers and sterilized by filtration using 0.22-μm filters (Millipore). Bacteria were collected from blood agar plates and resuspended in PBS at an optical density at OD_{600} of 1. Aliquots of 100 μl of bacterial suspensions (corresponding to 5×10^7 bacteria) were incubated with 100 μl of human saliva for 240 min at 37°C. As a negative control, 200 μl of 1:2-diluted human saliva solution alone was incubated for 240 min at 37°C. Samples were then centrifuged for 5 min at 13,000 × *g*, and supernatant collected and loaded in a 10% SDS gel. Samples were analyzed by lectin staining with PNA according to the manufacturer's recommendations (DIG glycan differentiation kit, catalog number 11210238001; Roche). MG2 mucin degradation was monitored by Western blotting with mouse anti human MG2 antibodies (ab55542; Abcam).

Mucinase assays with purified recombinant MucG. One hundred microliters of human saliva was incubated with 1 μg of purified MucG protein for 1.5 or 3.5 h at 37°C in the presence or absence of 50 mM EDTA. Samples were loaded onto 10% SDS-PAGE gels and analyzed by lectin staining with PNA according to the manufacturer's recommendations (DIG glycan differentiation kit; Roche).

Muc proteins copurification. *C. canimorsus* 5 Δ*mucC* bacteria harboring plasmid pFR26 expressing a C-terminal Strep-His double-tagged MucC, or harboring plasmid pFR27, expressing MucC without any tag (mock), were grown on sheep blood plates for 2 days at 37°C in the presence of 5% CO_2. Bacteria from 6 plates were scraped and lysed in 35 ml of 25 mM Tris-HCl, 150 mM NaCl, 0.2% Triton, 1% NP-40, 1% sodium deoxycholate, pH 7.6.

For His affinity purification, the lysates were clarified by centrifugation (10 min at 18,500 × *g* at room temperature), and the supernatant was diluted 1:2 in PBS, 10 mM imidazole in the presence of proteinase inhibitor (cOmplete Mini, EDTA-free protease Inhibitor cocktail tablets; Roche). Aliquots of 3.5 ml of a 50% slurry of chelating Sepharose fast flow beads (GE Healthcare) were first coupled to Ni^{2+} according to the manufacturer's instructions, and then 1.75 ml of resin was added to the solution and the mixture was incubated overnight at 4°C on a rotating wheel. The solution was then loaded into a column, and the resin was washed first with 25 column volumes (CV) of high-salt buffer (50 mM Tris, 500 mM NaCl; pH 8) and then with 5 CV of low-salt buffer (50 mM Tris, 100 mM NaCl; pH 8). Proteins were then eluted from the resin with 2 CV of elution buffer (50 mM Tris, 100 mM NaCl, 350 mM imidazole; pH 8). The material eluted from the Ni^{2+} column was then diluted 1:2 in PBS, and 1 ml of a 50% slurry (0.5 ml CV) of Strep-Tactin superflow resin (catalog number 2-1206-002; IBA) was added. The solution was then incubated overnight at 4°C on a rotating wheel. Next, the solution was loaded into a column, and the flowthrough was reloaded into the resin 2 more times. The resin was then washed 4 times with 10 CV of buffer W (100 mM Tris, 150 mM NaCl, 1 mM EDTA; pH 8), and proteins were eluted in 3 steps with 0.5 ml of elution buffer (100 mM Tris, 150 mM NaCl, 1 mM EDTA, 2.5 mM desthiobiotin; pH 8). Tagged MucC was detected by immunoblotting using mouse anti-His antibody (catalog number 27-4710-01; Amersham Bioscience), and the proteins present in the elution fractions were identified by LC/MS.

LC /MS identification of proteins in the elution fractions. Proteins eluted from the MucC-Strep-His and MucC (mock) pulldowns were separated on a 12% SDS gel. The proteins were silver stained and excised with a razor blade. Proteins were trypsin digested and analyzed by LC/MS as described in reference 15.

Phylogenetic analyses of $GlmU_{Cc}$. The orthologous cluster of KEGG: ml:Ccan_15070 ($GlmU_{Cc}$) was initially searched in the SSDB (KEGG) database within the bacterial kingdom with a best-best rule. Only hits above a threshold of 150 were further considered (137 hits). Because of low similarity levels between $GlmU_{Cc}$ and most of its bifunctional homologs, the cluster of orthologs was extended by searching the SSDB with the bifunctional GlmU ortholog, with the highest similarity score (i.e., the closest bifunctional relative of $GlmU_{Cc}$:dte:Dester_1461, 27% similarity). The second search clustered 2,403 hits (including ml:Ccan_15070). The two merged sets resulted in a cluster of 2,532 protein sequences that were submitted for Pfam domain identification (http://pfam.xfam.org/search#tabview=tab1). A total of 554 consensual 16S rRNA sequences (derived from 2 to 20,843 [*Bacillus*] individual sequences from the Ribosomal Database Project website [37]) from the genera identified here were used to determine a 16S rRNA-based phylogeny. The evolutionary history was inferred by using the neighbor-joining method (38). The bootstrap consensus tree inferred from 1,000 replicates (39) was taken to represent the evolutionary history of the taxa analyzed (40). Branches corresponding to partitions reproduced in less than 70% bootstrap replicates were collapsed. The analysis involved 554 nucleotide sequences. All positions with less than 50% site coverage were eliminated. That is, fewer than 50% alignment gaps, missing data, and ambiguous bases were allowed at any position. There were a total of 1,453 positions in the final data set. Evolutionary analyses were conducted with MEGA6 (41).

SUPPLEMENTAL MATERIAL

Supplemental material for this article may be found at http://mbio.asm.org/lookup/suppl/doi:10.1128/mBio.02507-14/-/DCSupplemental.

Figure S1, TIF file, 3 MB.

Figure S2, TIF file, 1.3 MB.
Figure S3, TIF file, 1.1 MB.
Figure S4, TIF file, 1 MB.
Movie S1, MOV file, 8.3 MB.
Movie S2, MOV file, 8.1 MB.
Table S1, DOCX file, 0.1 MB.
Table S2, DOCX file, 0.1 MB.
Table S3, DOCX file, 0.1 MB.
Table S4, DOCX file, 0.1 MB.

ACKNOWLEDGMENTS

We thank Frédéric Lauber for stimulating discussions.

We are grateful to Damien Hermand and Regis Hallez for assistance with the microscopy and to Paul Jenoe and Suzette Moes for LC/MS.

F.R. is a postdoctoral research fellow (Chargé de Recherche) of the Belgian Fonds National de la Recherche Scientifique. This work was financed by advanced grant 293605-CAPCAN from the European Research Council.

ADDENDUM IN PROOFS

During the reviewing process of this manuscript a paper was published in Nature (doi:10.1038/nature13995) showing that human gut Bacteroidetes can also utilize glycans via a selfish mechanism avoiding releasing polysaccharide breakdown products which could be utilized by competitor bacteria.

REFERENCES

1. **Brenner DJ, Hollis DG, Fanning GR, Weaver RE.** 1989. *Capnocytophaga canimorsus* sp. nov. (formerly CDC group DF-2), a cause of septicemia following dog bite, and *C. cynodegmi* sp. nov., a cause of localized wound infection following dog bite. J Clin Microbiol **27:**231–235.
2. **Shin H, Mally M, Meyer S, Fiechter C, Paroz C, Zaehringer U, Cornelis GR.** 2009. Resistance of *Capnocytophaga canimorsus* to killing by human complement and polymorphonuclear leukocytes. Infect Immun **77:**2262–2271. http://dx.doi.org/10.1128/IAI.01324-08.
3. **Blanche P, Bloch E, Sicard D.** 1998. *Capnocytophaga canimorsus* in the oral flora of dogs and cats. J Infect **36:**134. http://dx.doi.org/10.1016/S0163-4453(98)93918-4.
4. **Dilegge SK, Edgcomb VP, Leadbetter ER.** 2011. Presence of the oral bacterium *Capnocytophaga canimorsus* in the tooth plaque of canines. Vet Microbiol **149:**437–445. http://dx.doi.org/10.1016/j.vetmic.2010.12.010.
5. **Suzuki M, Kimura M, Imaoka K, Yamada A.** 2010. Prevalence of *Capnocytophaga canimorsus* and *Capnocytophaga cynodegmi* in dogs and cats determined by using a newly established species-specific PCR. Vet Microbiol **144:**172–176. http://dx.doi.org/10.1016/j.vetmic.2010.01.001.
6. **Bobo RA, Newton EJ.** 1976. A previously undescribed gram-negative bacillus causing septicemia and meningitis. Am J Clin Pathol **65:**564–569.
7. **Butler T, Weaver RE, Ramani TK, Uyeda CT, Bobo RA, Ryu JS, Kohler RB.** 1977. Unidentified gram-negative rod infection. A new disease of man. Ann Intern Med **86:**1–5. http://dx.doi.org/10.7326/0003-4819-86-1-1.
8. **Gaastra W, Lipman LJ.** 2010. *Capnocytophaga canimorsus*. Vet Microbiol **140:**339–346. http://dx.doi.org/10.1016/j.vetmic.2009.01.040.
9. **Janda JM, Graves MH, Lindquist D, Probert WS.** 2006. Diagnosing *Capnocytophaga canimorsus* infections. Emerg Infect Dis **12:**340–342. http://dx.doi.org/10.3201/eid1202.050783.
10. **Tierney DM, Strauss LP, Sanchez JL.** 2006. *Capnocytophaga canimorsus* mycotic abdominal aortic aneurysm: why the mailman is afraid of dogs. J Clin Microbiol **44:**649–651. http://dx.doi.org/10.1128/JCM.44.2.649-651.2006.
11. **Shin H, Mally M, Kuhn M, Paroz C, Cornelis GR.** 2007. Escape from immune surveillance by *Capnocytophaga canimorsus*. J Infect Dis **195:**375–386. http://dx.doi.org/10.1086/510243.
12. **Ittig S, Lindner B, Stenta M, Manfredi P, Zdorovenko E, Knirel YA, dal Peraro M, Cornelis GR, Zähringer U.** 2012. The lipopolysaccharide from *Capnocytophaga canimorsus* reveals an unexpected role of the core-oligosaccharide in MD-2 binding. PLoS Pathog **8:**e1002667. http://dx.doi.org/10.1371/journal.ppat.1002667.
13. **Zähringer U, Ittig S, Lindner B, Moll H, Schombel U, Gisch N, Cornelis GR.** 2014. NMR-based structural analysis of the complete rough-type lipopolysaccharide isolated from *Capnocytophaga canimorsus*. J Biol Chem **289:**23963–23976. http://dx.doi.org/10.1074/jbc.M114.571489.
14. **Manfredi P, Pagni M, Cornelis GR.** 2011. Complete genome sequence of the dog commensal and human pathogen *Capnocytophaga canimorsus* strain 5. J Bacteriol **193:**5558–5559. http://dx.doi.org/10.1128/JB.05853-11.
15. **Manfredi P, Renzi F, Mally M, Sauteur L, Schmaler M, Moes S, Jenö P, Cornelis GR.** 2011. The genome and surface proteome of *Capnocytophaga canimorsus* reveal a key role of glycan foraging systems in host glycoproteins deglycosylation. Mol Microbiol **81:**1050–1060. http://dx.doi.org/10.1111/j.1365-2958.2011.07750.x.
16. **Martens EC, Chiang HC, Gordon JI.** 2008. Mucosal glycan foraging enhances fitness and transmission of a saccharolytic human gut bacterial symbiont. Cell Host Microbe **4:**447–457. http://dx.doi.org/10.1016/j.chom.2008.09.007.
17. **Shipman JA, Berleman JE, Salyers AA.** 2000. Characterization of four outer membrane proteins involved in binding starch to the cell surface of *Bacteroides thetaiotaomicron*. J Bacteriol **182:**5365–5372. http://dx.doi.org/10.1128/JB.182.19.5365-5372.2000.
18. **Shipman JA, Cho KH, Siegel HA, Salyers AA.** 1999. Physiological characterization of SusG, an outer membrane protein essential for starch utilization by *Bacteroides thetaiotaomicron*. J Bacteriol **181:**7206–7211.
19. **Reeves AR, D'Elia JN, Frias J, Salyers AA.** 1996. A *Bacteroides thetaiotaomicron* outer membrane protein that is essential for utilization of maltooligosaccharides and starch. J Bacteriol **178:**823–830.
20. **Reeves AR, Wang GR, Salyers AA.** 1997. Characterization of four outer membrane proteins that play a role in utilization of starch by *Bacteroides thetaiotaomicron*. J Bacteriol **179:**643–649.
21. **Mally M, Shin H, Paroz C, Landmann R, Cornelis GR.** 2008. *Capnocytophaga canimorsus*: a human pathogen feeding at the surface of epithelial cells and phagocytes. PLoS Pathog **4:**e1000164. http://dx.doi.org/10.1371/journal.ppat.1000164.
22. **Renzi F, Manfredi P, Mally M, Moes S, Jenö P, Cornelis GR.** 2011. The N-glycan glycoprotein deglycosylation complex (Gpd) from *Capnocytophaga canimorsus* deglycosylates human IgG. PLoS Pathog **7:**e1002118. http://dx.doi.org/10.1371/journal.ppat.1002118.
23. **Manfredi P, Lauber F, Renzi F, Hack K, Hess E, Cornelis GR.** 2015. A new iron acquisition system in *Bacteroidetes*. Infect Immun **83:**300–310. http://dx.doi.org/10.1128/IAI.02042-14.
24. **Sarvas M.** 1971. Mutant of *Escherichia coli* K-12 defective in D-glucosamine biosynthesis. J Bacteriol **105:**467–471.
25. **Huang KC, Mukhopadhyay R, Wen B, Gitai Z, Wingreen NS.** 2008. Cell shape and cell-wall organization in gram-negative bacteria. Proc Natl Acad Sci U S A **105:**19282–19287. http://dx.doi.org/10.1073/pnas.0805309105.
26. **Boratyn GM, Schäffer AA, Agarwala R, Altschul SF, Lipman DJ, Madden TL.** 2012. Domain enhanced lookup time accelerated BLAST. Biol Direct **7:**12. http://dx.doi.org/10.1186/1745-6150-7-12.
27. **Barreteau H, Kovac A, Boniface A, Sova M, Gobec S, Blanot D.** 2008. Cytoplasmic steps of peptidoglycan biosynthesis. FEMS Microbiol Rev **32:**168–207. http://dx.doi.org/10.1111/j.1574-6976.2008.00104.x.
28. **Pompeo F, Bourne Y, van Heijenoort J, Fassy F, Mengin-Lecreulx D.** 2001. Dissection of the bifunctional *Escherichia coli N*-acetylglucosamine-1-phosphate uridyltransferase enzyme into autonomously functional domains and evidence that trimerization is absolutely required for glucosamine-1-phosphate acetyltransferase activity and cell growth. J Biol Chem **276:**3833–3839. http://dx.doi.org/10.1074/jbc.M004788200.
29. **Prakobphol A, Thomsson KA, Hansson GC, Rosen SD, Singer MS, Phillips NJ, Medzihradszky KF, Burlingame AL, Leffler H, Fisher SJ.** 1998. Human low-molecular-weight salivary mucin expresses the sialyl Lewis X determinant and has L-selectin ligand activity. Biochemistry **37:**4916–4927. http://dx.doi.org/10.1021/bi972612a.
30. **Nakjang S, Ndeh DA, Wipat A, Bolam DN, Hirt RP.** 2012. A novel extracellular metallopeptidase domain shared by animal host-associated mutualistic and pathogenic microbes. PLoS One **7:**e30287. http://dx.doi.org/10.1371/journal.pone.0030287.
31. **Mello LV, Chen X, Rigden DJ.** 2010. Mining metagenomic data for novel domains: BACON, a new carbohydrate-binding module. FEBS Lett **584:**2421–2426. http://dx.doi.org/10.1016/j.febslet.2010.04.045.
32. **Baumgartner S, Hofmann K, Chiquet-Ehrismann R, Bucher P.** 1998. The discoidin domain family revisited: new members from prokaryotes and a homology-based fold prediction. Protein Sci **7:**1626–1631. http://dx.doi.org/10.1002/pro.5560070717.
33. **Martens EC, Koropatkin NM, Smith TJ, Gordon JI.** 2009. Complex glycan catabolism by the human gut microbiota: the *Bacteroidetes* Sus-like paradigm. J Biol Chem **284:**24673–24677. http://dx.doi.org/10.1074/jbc.R109.022848.

34. **Xu J, Bjursell MK, Himrod J, Deng S, Carmichael LK, Chiang HC, Hooper LV, Gordon JI**. 2003. A genomic view of the human-*Bacteroides thetaiotaomicron* symbiosis. Science **299:**2074–2076. http://dx.doi.org/10.1126/science.1080029.
35. **Rakoff-Nahoum S, Coyne MJ, Comstock LE**. 2014. An ecological network of polysaccharide utilization among human intestinal symbionts. Curr Biol **24:**40–49. http://dx.doi.org/10.1016/j.cub.2013.10.077.
36. **Mally M, Cornelis GR**. 2008. Genetic tools for studying *Capnocytophaga canimorsus*. Appl Environ Microbiol **74:**6369–6377. http://dx.doi.org/10.1128/AEM.01218-08.
37. **Cole JR, Wang Q, Cardenas E, Fish J, Chai B, Farris RJ, Kulam-Syed-Mohideen AS, McGarrell DM, Marsh T, Garrity GM, Tiedje JM, Ribosomal Database Project**. 2009. Improved alignments and new tools for rRNA analysis. Nucleic Acids Res **37:**D141–D145. http://dx.doi.org/10.1093/nar/gkn879.
38. **Saitou N, Nei M**. 1987. The neighbor-joining method: a new method for reconstructing phylogenetic trees. Mol Biol Evol **4:**406–425.
39. **Felsenstein J**. 1985. Confidence limits on phylogenies: an approach using the bootstrap. Evolution **39:**783. http://dx.doi.org/10.2307/2408678.
40. **Tamura K, Nei M, Kumar S**. 2004. Prospects for inferring very large phylogenies by using the neighbor-joining method. Proc Natl Acad Sci U S A **101:**11030–11035. http://dx.doi.org/10.1073/pnas.0404206101.
41. **Tamura K, Stecher G, Peterson D, Filipski A, Kumar S**. 2013. MEGA6: molecular evolutionary genetics analysis version 6.0. Mol Biol Evol **30:**2725–2729. http://dx.doi.org/10.1093/molbev/mst197.